

Notice

This manuscript is peer-reviewed and accepted for publication in Geophysical Research Letters (manuscript #2020GL090827):

Title: Analytical prediction of seismicity rate due to tides and other oscillating stresses

Authors: Elias Rafn Heimisson (California Institute of Technology) (corr-auth), Jean-Philippe Avouac (California Institute of Technology)

DOI: 10.1029/2020GL090827

The version submitted to EarthArXiv is the final submitted version prior to acceptance and is made freely available here in compliance with AGU policies. The official published version and the EarthArXiv one differ slightly in copy editing, typesetting, and formatting, but not in terms of scientific content and results.

Contact: eheimiss@caltech.edu

1 **Analytical prediction of seismicity rate due to tides and**
2 **other oscillating stresses**

3 **Elías R. Heimisson¹, and Jean-Philippe Avouac¹**

4 ¹Division of Geological and Planetary Sciences, California Institute of Technology, Pasadena, CA, USA

5 **Key Points:**

- 6 • We derive a simple analytical model for seismicity rate based on rate-and-state
7 friction
- 8 • The model can be applied to perpetually oscillating stresses on earth and other
9 solid-surface bodies
- 10 • We reevaluate recent work on possible tidally triggered seismicity on Mars

Corresponding author: Elías R. Heimisson, eheimiss@caltech.edu

Abstract

Oscillatory stresses are ubiquitous on earth and other solid-surface bodies. Tides and seasonal signals perpetually stress faults in the crust. Relating seismicity to these stresses offers fundamental insight into earthquake triggering. We present a simple model that describes seismicity rate due to perpetual oscillatory stresses. The model applies to large amplitude, non-harmonic, and quasi-periodic stressing. However, it is not valid for periods similar to the characteristic time t_a . We show that seismicity rate from short-period stressing scales with the stress amplitude, but for long-periods with the stressing rate. Further, that background seismicity rate r is equal to the average seismicity rate during short-period stressing. We suggest $A\sigma_0$ may be underestimated if stresses are approximated by a single harmonic function. We revisit Manga et al. (2019), which analyzed the tidal triggering of Marsquakes, and provide a re-scaling of their seismicity rate response that offers a self-consistent comparison of different hydraulic conditions.

Plain Language Summary

The surface of Earth and many other planets and moons is constantly being stressed in an oscillatory manner, for example, by the gravitational pull of moons, planets, and suns. Further, weather, climate, oceans, and other factors may also generate oscillatory stresses. The resulting fluctuations in stress may result in an increased or decreased probability of earthquakes with time. Here we derive a simple formula that can help scientists understand how these oscillatory stresses relate to seismic activity. Moreover, we revisit a recent estimate of the maximum sensitivity of Marsquakes to tides and reach a different conclusion.

1 Introduction

Faults in the shallow crust are subject to perpetual, quasi-periodic, oscillatory stress perturbations due to several forcing factors. In particular, oceanic or solid-earth tides, seasonal surface loads due to surface hydrology and the cryosphere, and surface temperature changes. The study of the seismicity response to such stress variations can in principle provide insight into fault friction and earthquake nucleation mechanisms (e.g., Beeler & Lockner, 2003; Scholz et al., 2019; Luo & Liu, 2019; Ader et al., 2014) and possibly inform us of the preparatory phase to impending earthquakes (e.g., Chanard et al., 2019; S. Tanaka, 2012). Stresses from oscillatory loading are often temporally complex but can

42 be computed with reasonable accuracy (e.g., Tsuruoka et al., 1995; Agnew, 1997; Y. Tanaka
43 et al., 2015; Lu et al., 2018; Johnson et al., 2020), and their relationship to changes in
44 seismicity or tremor rate might reveal fundamental insight into earthquake triggering.
45 On Mars and the Moon, such factors might be the dominant source of seismicity (Manga
46 et al., 2019; Duennebier & Sutton, 1974; Lognonne, 2005).

47 Although earthquakes are often weekly correlated to tides, tectonic tremors seem
48 strongly correlated to tides both in the roots of strike-slip faults (Thomas et al., 2012,
49 2009) and subduction zones (Rubinstein et al., 2008; Yabe et al., 2015; Houston, 2015)
50 where slow-slip also is modulated by tidal stresses (Hawthorne & Rubin, 2010). Seasonal
51 variation of seismicity driven by surface load variations have been reported in several stud-
52 ies (e.g., Bettinelli et al., 2008; Amos et al., 2014; Ueda & Kato, 2019). However, in most
53 places, the seismicity rate depends weakly on tides (S. Tanaka et al., 2002; Cochran et
54 al., 2004), except at mid-ocean ridges (e.g., Tolstoy et al., 2002). With the emergence
55 of the next generation of machine learning and template matching techniques for gen-
56 erating earthquake catalogs, which may have ten times the sensitivity of traditional meth-
57 ods (e.g., Ross et al., 2019), we will be able to detect and quantify the seismicity response
58 to tidal and seasonal loading. New developments in observational earthquake seismol-
59 ogy, and the emplacement of a seismometer on Mars, call for a simple model for seismic-
60 ity rate under tidal loading that can be compared to data. Here we provide such a model
61 (equation 8) that can be readily used and has, in practice, only one free parameter in
62 most applications. Further, we highlight important assumptions, such as ignoring finite
63 fault effects and discuss potential pitfalls in applying rate-and-state seismicity produc-
64 tion models to oscillatory stresses.

65 Theoretical studies have used the rate-and-state seismicity production model of Dieterich
66 (1994) to develop an approximate theory for oscillatory stresses. Dieterich (2007) rec-
67 ognized that for small amplitude and short duration stress changes, the tidally induced
68 signal could be approximated as the instantaneous response predicted by the Dieterich
69 (1994) theory. Under these assumptions, Dieterich (2007) derived a simple relationship
70 for a harmonic stress perturbation. Ader et al. (2014) provided a more general analyt-
71 ical expression; however, the analysis of Ader et al. (2014) was also restricted to a sin-
72 gle harmonic perturbation. Because rate-and-state friction is non-linear, knowing the re-
73 sponse to harmonic perturbations is not sufficient to describe the response to oscillatory
74 stress variations in general. For example, tidal loading cannot be explained by a single

75 harmonic perturbation (e.g., Figure 1), and the formalism of Dieterich (2007) and Ader
 76 et al. (2014) would not allow estimating the expected seismicity response. We, therefore,
 77 present a simple approximate relationship for seismicity rate due to arbitrary long-term
 78 oscillatory stressing that is superimposed on the long-term constant stressing rate. The
 79 oscillatory stressing can be non-harmonic, quasi-periodic, and include random variations.
 80 The approximation is valid as long as the average of the oscillatory stress converges to
 81 a mean value on a time-scale shorter than a characteristic time t_a . We give a mathemat-
 82 ical condition for when the approximation is valid and provide corrections and alterna-
 83 tive expressions for end-member cases where the approximation breaks down. As an il-
 84 lustration, we revisit the analysis of the seismicity response to tidal forcing on Mars of
 85 Manga et al. (2019), based on the solution of Dieterich (1994).

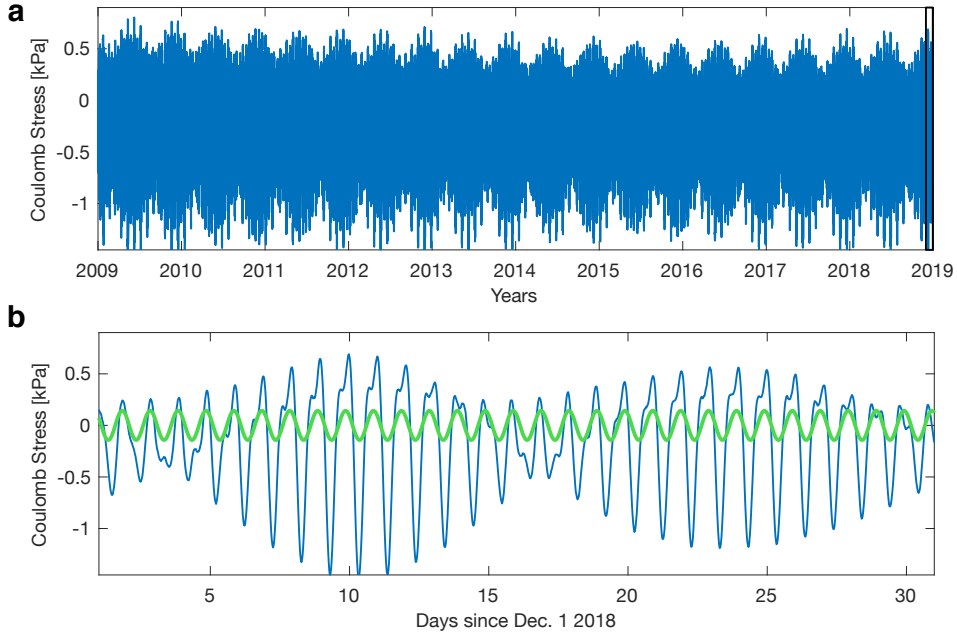


Figure 1. Time-series of Coulomb stress changes due to the solid earth tides. **a** 10 years of Coulomb stress perturbations due to solid earth tides on a shallow right-lateral strike-slip fault striking NW-SE and located at Caltech campus. **b** The stress changes in the black box in **a** in blue, green represents the dominant single harmonic mode of the Coulomb stress time series. In section 3.1 we will compute the theoretical seismicity rate during the period in **b** where the entire time-series in **a** is used to fade out the instantaneous initial response.

2 Theory

In this section, we present a simple model for triggering due to oscillatory stresses. We refer the reader to Appendix A for the details of the derivation.

Heimisson and Segall (2018) re-derived the Dieterich (1994) theory and showed:

$$R(t) = r \frac{K(t)}{1 + \frac{1}{t_a} \int_0^t K(t') dt'}, \quad (1)$$

where $R(t)$ is the seismicity rate produced by a population of seismic sources with background seismicity rate r . Further, $t_a = A\sigma_0/\dot{s}_0$ is a characteristic time over which fluctuations in seismicity rate return to the background seismicity and A is a constitutive parameter proportional to the instantaneous frictional dependence on rate. If changes in normal stress $\sigma(t)$ are small compared to the initial normal stress σ_0 then K is well approximated as:

$$K(t) \approx \exp\left(\frac{S(t)}{A\sigma_0}\right). \quad (2)$$

However, see equation 30 in Heimisson and Segall (2018) for detailed conditions. $S(t) = \tau(t) - \mu\sigma(t)$ and $\dot{s}_0 = \dot{\tau}_r - \mu\dot{\sigma}_r$ are the modified Coulomb stressing history and background stressing rate respectively with $\mu = \tau_0/\sigma_0 - \alpha$ where α is the Linker and Dieterich (1992) constant, typically between 0 – 0.25 and describes coupling of normal stress and state. It is worth emphasizing that μ does thus not represent a coefficient of friction in the traditional sense; hence the name modified Coulomb stress.

The population of seismic sources is assumed to be non-interacting; however, Heimisson (2019) showed that an interacting population could be modeled as an equivalent non-interacting population. This means that we don't expect interaction on average to fundamentally change the response of the system to perturbations.

The presence of the integral in equation 1 and the fact that $K(t) > 0$ causes perturbations introduced at $t = 0$ to decay. The short time limit of equation 1, when the integral is much smaller than t_a , is the instantaneous response due to a perturbation in stress:

$$R = rK(t) \approx r \exp\left(\frac{S(t)}{A\sigma_0}\right). \quad (3)$$

110 Dieterich (2007) argued that the instantaneous response (equation 3) is appropriate for
 111 periodic loading when the period T is small compared to a characteristic time, which de-
 112 scribes when the seismicity rate starts decaying, in other words, the onset of the "Omori"
 113 ($\sim 1/t$) decay following a step change in stress. In Appendix A, we investigate the va-
 114 lidity of that argument by Dieterich (2007), which has often been applied the tidal trig-
 115 gering of seismicity and tremor (e.g., Dieterich, 2007; Thomas et al., 2012; Delorey et
 116 al., 2017; Scholz et al., 2019). In Appendix A, we show for a time-dependent stressing
 117 history of the form $S(t) = S_T(t) + \dot{s}_0 t$, where $S_T(t)$ is an oscillatory modified coulomb
 118 stress with a well defined average value (e.g., tidally induced stress), the long term re-
 119 sponse in seismicity rate is:

$$\frac{R(t)}{r} = \frac{\exp\left(\frac{S_T(t)}{A\sigma_0}\right)}{M}, \quad (4)$$

120 where M is the average

$$M = \lim_{T \rightarrow \infty} \frac{1}{T} \int_0^T \exp\left(\frac{S_T(t)}{A\sigma_0}\right) dt. \quad (5)$$

121 We note that $M = 1$ only if $S_T(t) = 0$. The average of $S_T(t)$ may be zero, but
 122 with non-zero amplitude, we always have $M > 1$. Equation 4 generalizes the special
 123 cases for a harmonic perturbation that was explored by Ader et al. (2014). One impor-
 124 tant consequence of equations 4 and 5 is that the average seismicity rate $\bar{R}(t)$ under os-
 125 cillatory stresses is the same as the background rate r when no oscillatory stresses oc-
 126 cur. This can be shown explicitly:

$$\frac{\bar{R}(t)}{r} = \lim_{T \rightarrow \infty} \frac{1}{T} \int_0^T \frac{R(t)}{r} dt = \frac{1}{M} \lim_{T \rightarrow \infty} \frac{1}{T} \int_0^T \exp\left(\frac{S_T(t)}{A\sigma_0}\right) dt = 1. \quad (6)$$

127 In other words, in the presence of general oscillatory stresses, the background rate, in
 128 the traditional sense expressed by Dieterich (1994), is observable as the average seismic-
 129 ity rate. This finding is consistent with equation 55 derived by Helmstetter and Shaw
 130 (2009), which shows that earthquake number is linearly proportional to the stress change
 131 at $t \gg t_a$ and thus a zero mean stress change would not induce any change in a num-
 132 ber of events, for an observation time much longer than t_a . However, equation 6 is more
 133 general since it doesn't assume that the mean stress is zero.

134 Let's define t_0 as a zero-crossing time of the oscillatory stress perturbation, i.e., $S_T(t_0) =$
 135 0. Then the rate is

$$R_0 = \frac{r}{M}. \quad (7)$$

136 It can thus be useful to rewrite equation 4

$$R(t) = R_0 \exp\left(\frac{S_T(t)}{A\sigma_0}\right). \quad (8)$$

137 Rate R is equal to the background average rate r when there are no oscillatory stresses
 138 (that is $R_0 = r$ if $M = 1$), thus the approximation proposed by Dieterich (2007) (equa-
 139 tion 3) is valid when the stress perturbation is very small compared to $A\sigma_0$ ($|S_T(t)|/A\sigma_0 \ll$
 140 1); otherwise, it remains valid within a scaling factor M . If $M > 1$ the peak-to-peak
 141 variation of the seismicity can be significantly overestimated. For many applications, the
 142 assumption $|S_T(t)|/A\sigma_0 \ll 1$ is valid. In applications to aftershocks $A\sigma_0 \sim 0.01 - 0.1$
 143 MPa (Hainzl, Steacy, & Marsan, 2010), which is much larger than tidal stresses ($\sim 10^{-3} - 10^{-4}$
 144 MPa, e.g., Figure 1). However, tidal triggering of tectonic tremors near Parkfield has sug-
 145 gested an average value of $A\sigma_0 = 6 \cdot 10^{-4}$ MPa (Thomas et al., 2012), in which case
 146 $S_T(t)/A\sigma_0$ could be on the order of 0.2 - 2. So the $S_T(t)/A\sigma_0 \ll 1$ assumption is clearly
 147 violated. Furthermore, $A\sigma_0$ may be generally different on other planetary bodies com-
 148 pared to earth (Manga et al., 2019).

149 It is useful to summarize the fundamental underlying assumptions that give rise
 150 to equation 4 or 8:

- 151 1. The average in equation 5 should converge on a time-scale much less t_a .
- 152 2. Oscillatory stresses $S_T(t)$ have been ongoing for a time much larger than t_a .
- 153 3. Normal stress changes should be modest compared to initial normal stress for the
 154 Coulomb stress approximation to be valid (Heimisson & Segall, 2018).
- 155 4. Other assumptions of the Dieterich (1994) theory, most importantly, source finite-
 156 ness can be neglected (see Kaneko & Lapusta, 2008), the population of seismic sources
 157 is well above steady-state (see Heimisson & Segall, 2018), and neglecting effects
 158 that arise from source interactions (see Heimisson, 2019).

159 Additional discussion of these assumptions is provided in Appendix A and Appendix
 160 B, but it is worth highlighting here a fundamental difference that arises when the pe-

161 riod of oscillations is much larger than t_a , and assumption 1 is strongly violated, in which
 162 case the seismicity rate is proportional to the stressing rate, not the stress:

$$\frac{R(t)}{r} \approx \frac{1}{1 - t_a \frac{\dot{S}_T(t)}{A\sigma_0}}. \quad (9)$$

163 One can interpret equation 9 such that long period stresses effectively change the
 164 background rate to $r'(t) = r/(1 - t_a \dot{S}_T(t)/(A\sigma_0))$ because the populations of seismic
 165 sources can evolve to a new steady-state rate on time-scales larger than t_a . In Appendix
 166 B we show how a combination of 4 and 9 can be used when long period and short pe-
 167 riod stressing is superimposed (see. equation B6).

168 3 Examples of applications and comparison with theory

169 3.1 Application to solid-earth tides

170 To test equation 4 against the full solution (equation 1) we generate a time series
 171 of Coulomb stress change using the *Solid* software (Milbert, 2018) representing the (mod-
 172 ified) Coulomb stress changes, with $\mu = 0.4$, due to the solid earth tides on shallow right-
 173 lateral strike-slip fault striking NW-SE and located at Caltech campus in California. The
 174 entire time-series is shown in Figure 1a, but we will restrict our attention to the obser-
 175 vation window shown in Figure 1b. Most of the time series in Figure 1a is used to erase
 176 the initial response or initial conditions in equation 1 and compute M . In the following
 177 we refer to this procedure simply as erasing the initial response. We choose $t_a = 0.5$
 178 years. We vary $A\sigma_0$ as described in Figure 2 choosing values that reflect a typical range
 179 of values in aftershock studies: 0.1 and 0.01 MPa (Hainzl, Steacy, & Marsan, 2010) and
 180 a value inferred in studying tidal triggering of tectonic tremors $6 \cdot 10^{-4}$ MPa (Thomas
 181 et al., 2012). We find that even for large fluctuations in R/r , equation 4 is in good agree-
 182 ment with the full solution (Figure 2c).

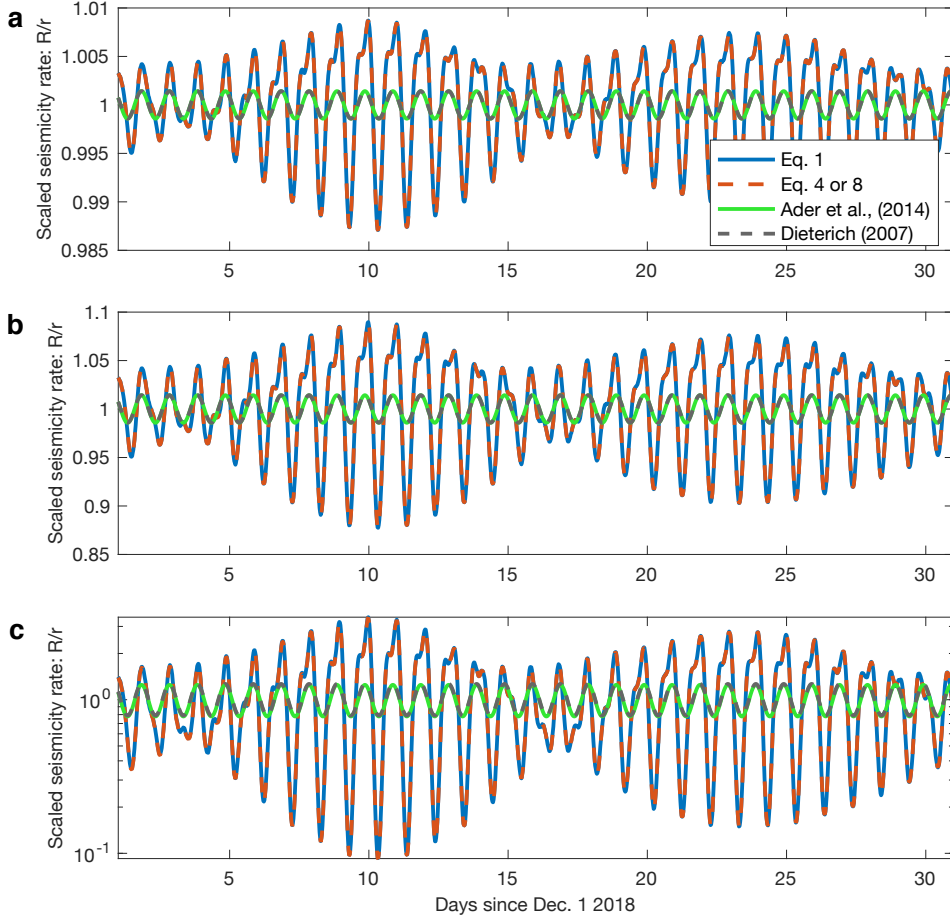


Figure 2. Comparison of various approximations and the full solution in equation 1 after the initial response has been faded out. Scaled seismicity rate (R/r) for (a) $A\sigma_0 = 1 \cdot 10^{-1}$ MPa, (b) $A\sigma_0 = 1 \cdot 10^{-2}$ MPa, (c) $A\sigma_0 = 6 \cdot 10^{-4}$ MPa (note the logarithmic scale). In all cases equation 4 provides an excellent approximation in all cases with an average relative error of less than 0.002 %, 0.02 %, and 0.7 % in panels a, b, and c respectively. A single harmonic perturbation does not capture the details of the curve shape or amplitude.

183 Corresponding theory for a single harmonic stress perturbation of Dieterich (2007)
 184 is obtained from equation 3 by representing $S_T(t)$ by a single harmonic function. Like-
 185 wise, the harmonic theory of Ader et al. (2014) is obtained in the same manner from equa-
 186 tion 4. We computed the dominant frequency of the signal in Figure 1a by computing
 187 a power spectral density. Then find the best fitting amplitude and phase by minimiz-
 188 ing an L_2 norm that quantifies the residual between the time-series shown in Figure 1a
 189 and the single harmonic function. The resulting harmonic stress perturbation is shown

190 in Figure 1b in green used to compute the seismicity rate using both the expressions from
191 Dieterich (2007) and Ader et al. (2014) in Figure 2. The dominant frequency of the earth-
192 tide signal generally predicts when the seismicity rate is higher or lower than average.
193 However, the shape and amplitude of the theoretical seismicity rate time-series cannot
194 be matched with a single harmonic function.

195 **3.2 Marsquakes: Reevaluating Manga et al. (2019)**

196 Recently, Manga et al. (2019) argued that Mars might have a clearer relationship
197 between tides and seismicity rate, which could result in variation as large as two orders
198 of magnitude in scaled seismicity rate R/r , also referred to as relative seismicity rate (see
199 Figure 3 bottom-left panel in Manga et al. (2019)). Their predicted signal was appar-
200 ently produced based on the initial instantaneous response (Figure 3a) and thus not strictly
201 correct, as presented. As discussed in the previous section, care needs to be taken to erase
202 the initial response when applying equation 1 by simulating a time window before the
203 observation window that is much larger than t_a and is sufficiently long to estimate M
204 accurately. If this is not done, the tidal response may be significantly over-estimated, in-
205 deed by a factor of $1/M$.

206 We use equation 1 without erasing the initial response and find a good agreement
207 with their results (Figure 3a), despite some simplifying assumptions that are detailed
208 in the next paragraph. Extrapolation of their results suggests that the changes in seis-
209 micity rate should be much smaller than they estimated (Figure 3b).

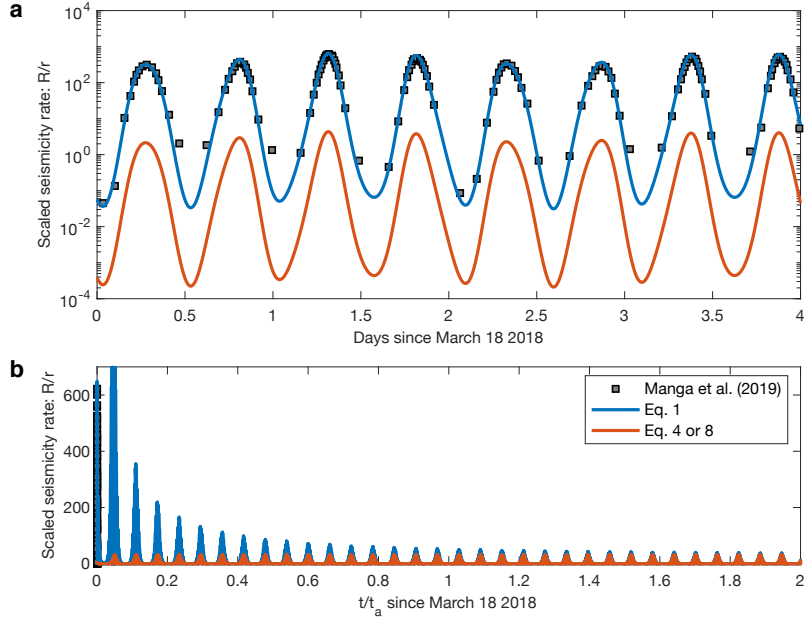


Figure 3. Reevaluation of Manga et al. (2019), reveals that they likely overestimated the maximum response by at least a factor of 10. (a) Using an approximate stressing history we observe that equation 1 is in good agreement with the results reported in Figure 3 bottom-left panel in Manga et al. (2019). In contrast, equation 4 suggests that the amplitude should be approximately 100 times less although the shape of the curves is the same. (b) Simulating a time-scale $t \sim t_a$ where $t_a \approx 71.5$ earth years, which we computed based on parameters given by Manga et al. (2019), shows that equation 1 and 4 converge once the initial response gets erased.

210 To replicate the results of Manga et al. (2019), we approximate the Coulomb stress
 211 perturbations they reported for strike = 0° (Figure 2 in Manga et al. (2019)) by a sum
 212 of three harmonic functions fitted to a digitized version of their figure. This provides an
 213 excellent fit to the reported Coulomb stress calculations during the four days window
 214 they show. However, the long term extrapolation in Figure 3b shows that the seismic-
 215 ity rate decays over a time-scale of $t \sim t_a$, before reaching the expected rate variation
 216 due to tidal loading that would be observable.

217 Fortunately, the ratio between the instantaneous response and the long-term re-
 218 sponse is M . Thus from equation 8 we can conclude that the reported relative rate of
 219 Manga et al. (2019) is correct if interpreted as relative to R_0 , but not r as they stated.
 220 One important consequence is that the difference in seismicity rate shown in different
 221 panels in Figure 3 in Manga et al. (2019) (showing response due to variations in effec-

222 tive normal stress) does not reflect relative changes in absolute seismicity rate. In their
 223 top panels $M \approx 1$, in the bottom panels $M \approx 100$. The maximum rate in the bottom
 224 panel is ≈ 600 , but for the top ≈ 1 . Thus, the difference in maximum absolute seismic-
 225 ity rate, of the two scenarios, is only about a factor of 6.

226 4 Discussion

227 Equations 4 or 8 offer an estimate of the seismicity rate produced by a population
 228 of seismic sources due to a stressing history produced by a constant stressing rate and
 229 oscillating stress sources. These equations are perfectly equivalent and simple to use, given
 230 that the stressing history is known, there is only one free parameter that may need to
 231 be fitted: $A\sigma_0$. The results thus offer a way to assess the validity rate-and-state seismic-
 232 ity rate theories (Dieterich, 1994; Heimisson & Segall, 2018) and place constraints on the
 233 friction law. Further, estimating $A\sigma_0$ by using tides or seasonal stress variations has im-
 234 plications for physics-based forecasts of aftershocks, where this parameter also needs to
 235 be estimated (e.g. Hainzl, Brietzke, & Zoller, 2010). Thus tides could be used in advance
 236 to or map spatial variations of this parameter. Those values could then be used for af-
 237 tershock forecasts once an earthquake occurs or forecast induced seismicity expected in
 238 response to anthropogenic stress changes.

239 Equation 8 may be preferred in some data applications compared to equation 4.
 240 Remarkably, Yabe et al. (2015) and Scholz et al. (2019) successfully applied equation 8
 241 in good agreement with data without explicit theoretical underpinnings. While Yabe et
 242 al. (2015) correctly state that R_0 is a reference rate when tidal stress is zero, the latter
 243 study refers to R as "the instantaneous seismicity rate". We have shown here that R in
 244 equation 3 represents the instantaneous seismicity rate, but equation 8 is the approx-
 245 imate seismicity rate in the presence of long term response tidal loading or other oscil-
 246 latory stresses. $R_0 \neq r$, unless $|S_T(t)|/A\sigma_0 \ll 1$ for all t , in which case $R_0 \approx r$.

247 The approximation made in equation 4 or 8 is not valid in the limit of a very long
 248 period stress variations that are larger than t_a , as described by equation 9. In this case,
 249 we expect the seismicity rate to be proportional to the stressing rate, but not the stress.
 250 Beeler and Lockner (2003) conducted experiments on a saw-cut sample in a triaxial load-
 251 ing frame. They imposed oscillatory stresses on a constant stressing rate and found that
 252 for short periods compared to the nucleation time, changes in event probability was in

253 phase with the stress. However, for long periods the probability of events was propor-
 254 tional to and in phase with the stressing rate. Their finding is in agreement with our the-
 255 oretical results.

256 Johnson et al. (2017) investigated the relationship between seismicity rate and sea-
 257 sonal variations in shear stress and stress rate in California. Depending on fault orien-
 258 tation, they identified a weak correlation of seismicity rate with either shear stressing
 259 rate or stress. This finding would suggest that, on average, t_a changes with fault orien-
 260 tation. That is reasonable since background stressing rates must vary with fault orien-
 261 tation. We emphasize that when investigating seasonal changes in seismicity rate, which
 262 may be on a similar time-scale as t_a , one must be careful since no approximation pre-
 263 sented here may work. We strongly suggest that equation 1 should be used for reference
 264 after erasing the initial response. Further, we recall that our analysis assumes that a sin-
 265 gle degree of freedom spring-and-slider system can approximate the response of a fault
 266 to a stress perturbation. Significant differences have been observed if finite fault effects
 267 need to be taken into account (e.g. Kaneko & Lapusta, 2008; Ampuero & Rubin, 2008;
 268 Rubin & Ampuero, 2005). Simulations indicate that this happens if the typical period
 269 of the stress perturbation is of the order of $2\pi t_a$ (Ader et al., 2014). In that case, the
 270 approximate analytical solutions described in this study would not apply.

271 Using a single harmonic function to represent the oscillating stressing history may
 272 be desirable due to the simplicity of the problem and the fact that spectral analysis, such
 273 as the Schuster spectra, can be used to extract the dominant period of the seismicity rate
 274 (Ader et al., 2014). However, this may lead to a bias in the estimate of $A\sigma_0$ if the stress-
 275 ing history has multiple components that can add up coherently. Let us assume that the
 276 stressing history is composed of N harmonic components:

$$S_T(t) = \sum_{i=1}^N c_i \sin\left(\frac{2\pi t}{T_i} + \phi_i\right) \quad (10)$$

277 where the amplitudes are sorted: $c_1 > c_2 > \dots > c_N$ and thus T_1 is the dominant pe-
 278 riod. Using equation 8 and only the dominant harmonic component of the $S_T(t)$ then
 279 one finds:

$$\log\left(\frac{\max(R)}{R_0}\right) = \frac{c_1}{(A\sigma_0)_{SH}}, \quad (11)$$

280 where $(A\sigma_0)_{SH}$ represent the estimate of $A\sigma_0$ under the assumption of a single harmonic,
 281 and $\max(R)$ is the maximum observed seismicity rate. However, for multiple harmon-
 282 ics we find:

$$\log\left(\frac{\max(R)}{R_0}\right) = \max\left(\frac{\sum_{i=1}^N c_i \sin\left(\frac{2\pi t}{T_i} + \phi_i\right)}{(A\sigma_0)_{MH}}\right) \leq \frac{\sum_{i=1}^N |c_i|}{(A\sigma_0)_{MH}}, \quad (12)$$

283 where $(A\sigma_0)_{MH}$ represents the estimate of $A\sigma_0$ under the assumption of multiple har-
 284 monics. Thus we conclude that the ratio of the two estimates is bounded in the follow-
 285 ing manner:

$$\frac{(A\sigma_0)_{MH}}{(A\sigma_0)_{SH}} \leq \frac{\sum_{i=1}^N |c_i|}{|c_1|}. \quad (13)$$

286 Therefore, we expect that $A\sigma_0$ is typically underestimated if a single harmonic stress source
 287 is assumed. This conclusion is consistent with Figure 2, which shows that the amplitude
 288 is not well match by a single harmonic. However, dividing $A\sigma_0$ by factor 5.3 would al-
 289 low the single harmonic approximation to match the maximum rate of the full solution.
 290 Equation 13 thus successfully offers an inequality constraint of $(A\sigma_0)_{MH} \leq 30 \cdot (A\sigma_0)_{SH}$.

291 5 Conclusions

292 We have derived a simple approximate equation to quantify the relationship be-
 293 tween seismicity and oscillatory stresses, based on assuming an earthquake nucleation
 294 process governed by rate-and-state friction. This relationship may be used, for exam-
 295 ple, in theoretical or observational studies of seismicity response to tidal and seasonal
 296 loading. For stress perturbations with periods shorter than t_a equation 4 or 8 provide
 297 an excellent approximation. We have also provided an approximation for periods longer
 298 than t_a (equation 9). Finally, in Appendix B and equation B6 we offer an approxima-
 299 tion for superposition of short period loading and long period loading relative to t_a . How-
 300 ever, for stress perturbations with periods $\sim t_a$ require a more careful analysis (e.g. equa-
 301 tion 1).

302 Acknowledgments

303 This is a theoretical paper and contains no data. This research was partly supported by
 304 NSF award EAR-1821853. We thank three anonymous reviewers for their constructive
 305 remarks that significantly improved this manuscript.

306 **Appendix A Derivation of equation 4**

307 We write the stressing history as the sum of steady stressing rate ($\dot{s}_0 t$) and time-
 308 dependent stress perturbation $S_T(t)$, i.e. $S(t) = S_T(t) + \dot{s}_0 t$ and obtain

$$K(t) = \exp\left(\frac{S(t)}{A\sigma_0}\right) = \exp\left(\frac{S_T(t)}{A\sigma_0} + \frac{t}{t_a}\right) = \eta(t) \exp\left(\frac{t}{t_a}\right). \quad (\text{A1})$$

309 We assume $\eta(t)$ is a function with the following property

$$\eta(t) = M + \epsilon(t), \text{ where } M = \lim_{T \rightarrow \infty} \frac{1}{T} \int_0^T \eta(t) dt \text{ with } |M| < \infty, \quad (\text{A2})$$

310 it follows that

$$\lim_{T \rightarrow \infty} \frac{1}{T} \int_0^T \eta(t) dt = \lim_{T \rightarrow \infty} \frac{1}{T} \int_0^T M dt + \frac{1}{T} \int_0^T \epsilon(t) dt = M + \lim_{T \rightarrow \infty} \frac{1}{T} \int_0^T \epsilon(t) dt. \quad (\text{A3})$$

311 In other words, M is the average of $\eta(t)$ and $|M| < \infty$; thus the average of $\epsilon(t)$ is zero,
 312 that is

$$\lim_{T \rightarrow \infty} \frac{1}{T} \int_0^T \epsilon(t) dt = 0. \quad (\text{A4})$$

313 For example, any periodic bounded function $\eta(t) = \eta(t+T)$, satisfies these conditions.

314 In this case, the physical interpretation of $\eta(t)$ is $\log(\eta(t)) = S_p(t)/A\sigma_0$ where $S_p(t) =$
 315 $S_p(t+T)$ is a periodic stress perturbation.

316 There is no requirement that $S_T(t)$ has to be a harmonic perturbation, such as pre-
 317 viously explored (Ader et al., 2014; Dieterich, 2007), or a periodic perturbation. Tidal
 318 loading has multiple harmonic components and their periods do not exactly differ by an
 319 integer. The resulting stressing history is not periodic. However, we can still write $\eta(t) =$
 320 $\exp(S_T(t)/A\sigma_0) = M + \epsilon(t)$. Further, we could imagine that $\epsilon(t)$ contains a stochastic
 321 component with a well defined mean. We shall now derive the long term behavior of a
 322 population of seismic sources that is persistently subject to a stressing history that can
 323 be written in the form of equation A1.

324 Once the integral in the denominator of equation 1 is much larger than t_a we may
 325 simplify

$$\frac{R(t)}{r} = \frac{K(t)}{\frac{1}{t_a} \int_0^t K(t') dt'}, \quad (\text{A5})$$

326 or using the notation in equation A1

$$\frac{R(t)}{r} = \frac{\eta(t) \exp\left(\frac{t}{t_a}\right)}{\frac{1}{t_a} \int_0^t \eta(t') \exp\left(\frac{t'}{t_a}\right) dt'}. \quad (\text{A6})$$

327 Substitution with A2 yields

$$\int_0^t \eta(t') \exp\left(\frac{t'}{t_a}\right) dt' = t_a M \exp\left(\frac{t}{t_a}\right) + \int_0^t \epsilon(t') \exp\left(\frac{t'}{t_a}\right) dt' \quad (\text{A7})$$

328 and we obtain:

$$\frac{R(t)}{r} = \frac{\eta(t)}{M + \frac{1}{t_a} \int_0^t \epsilon(t') \exp\left(\frac{-(t-t')}{t_a}\right) dt'}. \quad (\text{A8})$$

329 We recognize that $\int_0^t \epsilon(t') \exp\left(\frac{-(t-t')}{t_a}\right) dt'$ is simply a convolution. The function $\exp(-(t-t')/t_a)$,
 330 imposes a memory effect and essentially eliminates any contribution in fluctuations in
 331 $\epsilon(t)$ in a time window of that lies significantly outside times $t-t_a$ to t . Thus if $\epsilon(t)$ av-
 332 erages to 0 on a time-scale that is significantly shorter than t_a the integral can gener-
 333 ally be ignored. For example, this condition is satisfied if the oscillatory stresses and pos-
 334 sible random stresses, average to approximately zero on a time-scale smaller than t_a . More
 335 precisely, the integral can be ignored if the following condition applies:

$$\left| \frac{\frac{1}{t_a} \int_0^t \epsilon(t') \exp\left(\frac{-(t-t')}{t_a}\right) dt'}{M} \right| \ll 1, \text{ for all } t, \quad (\text{A9})$$

336 then equation A8 reduces to

$$\frac{R(t)}{r} = \frac{\eta(t)}{M} = \frac{\exp\left(\frac{S_T(t)}{A\sigma_0}\right)}{M}. \quad (\text{A10})$$

337 **Appendix B Validity of equations 4/8**

338 Here we offer further analysis on the validity of equation 4 or 8 and provide some
 339 insight into the regimes when they are not valid. The validity of equation 4 or 8 rests
 340 on the validity of equation A9. We investigate two different expansions of the relevant
 341 term through repeated integration by parts:

$$\frac{1}{t_a} \exp\left(-\frac{t}{t_a}\right) \int \epsilon(t') \exp\left(\frac{t'}{t_a}\right) dt' = \frac{\epsilon^{-1}(t)}{t_a} - \frac{\epsilon^{-2}(t)}{t_a^2} + \frac{\epsilon^{-3}(t)}{t_a^3} + \dots \quad (\text{B1})$$

$$\frac{1}{t_a} \exp\left(-\frac{t}{t_a}\right) \int \epsilon(t') \exp\left(\frac{t'}{t_a}\right) dt' = \epsilon - t_a \epsilon^1(t) + t_a^2 \epsilon^2(t) - t_a^3 \epsilon^3(t) + \dots \quad (\text{B2})$$

342 where ϵ^n is the n -th derivative of ϵ and ϵ^{-n} is the n -th indefinite integral (or anti-derivative)
 343 of ϵ . If the largest period, T_{max} in the Fourier decomposition of ϵ with a non-zero co-
 344 efficient satisfies $T_{max} < t_a$ then the n -th term in equation B1 will be a correction of
 345 order $O(T_{max}^n/t_a^n)$, and convergence is expected. For long period changes $T_{min} > t_a$,
 346 equation B2 provides an expansion where we have $O(t_a^n/T_{min}^n)$ correction for the n -th
 347 term.

348 In the short period limit, $T_{max} < t_a$, we find a first-order correction to equation
 349 4:

$$\frac{R(t)}{r} = \frac{\exp\left(\frac{S_T(t)}{A\sigma_0}\right)}{M + \frac{\epsilon^{-1}(t)}{t_a}}, \quad (\text{B3})$$

350 where in practice we compute $\epsilon^{-1}(t)$ using the following equation unless the indefinite
 351 integral is known analytically.

$$\epsilon^{-1}(t) = \int_{-t_0}^t \exp\left(\frac{S_T(t)}{A\sigma_0}\right) dt - Mt, \quad (\text{B4})$$

352 where $t_0 > 0$ is chosen sufficiently large to erase the influence of the initial stress value
 353 in the integral. Numerical exploration of equation B3 suggested that the additional cor-
 354 rection term is typically small and unlikely to be useful in practical applications.

355 In the long period limit, $T_{min} > t_a$, we get,

$$\frac{R(t)}{r} = \frac{\exp\left(\frac{S_T(t)}{A\sigma_0}\right)}{\exp\left(\frac{S_T(t)}{A\sigma_0}\right) - t_a \exp\left(\frac{S_T(t)}{A\sigma_0}\right) \frac{\dot{S}_T(t)}{A\sigma_0}} = \frac{1}{1 - t_a \frac{\dot{S}_T(t)}{A\sigma_0}} \approx 1 + t_a \frac{\dot{S}_T(t)}{A\sigma_0}, \quad (\text{B5})$$

356 where the approximation represents a first order Taylor expansion. Equation B5 may
 357 be useful when investigating long term behavior such as seasonal changes if t_a is shorter
 358 than 1 year as is probably the case in active tectonic settings (e.g. Bettinelli et al., 2008).
 359 Notably, equation 9 depends on the stressing rate, not directly the stress, and is to the

360 first order linearly proportional to the stressing rate (Figure B1). Implying that, in this
 361 particular limit, the seismicity rate is out of phase with the stress variations. This re-
 362 sult is consistent with the findings of Helmstetter and Shaw (2009) for slowly varying
 363 stresses. Furthermore, we see that equation 4 is not valid in this limit since it predicts
 364 that the seismicity rate is proportional to the stress change, not the stressing rate.

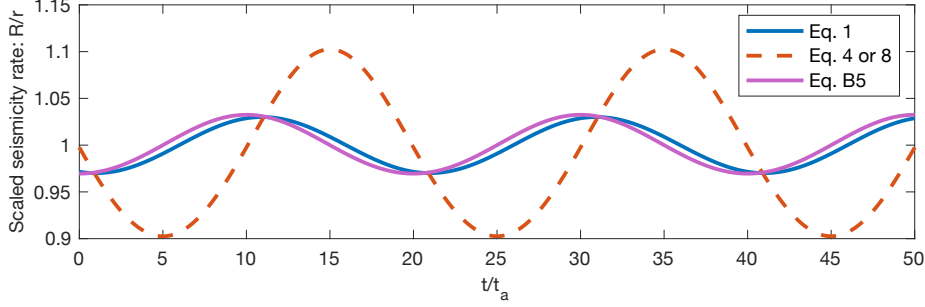


Figure B1. Simulations of seismicity rate response for $S_T(t)/A\sigma_0 = -0.1 \cdot \sin(2\pi t/T) + t/t_a$, where the period $T = 20t_a$. In this limit equation 9 predicts that the seismicity rate should be in phase the stressing rate and the equations 4 or 8 are in no agreement with the full solution 1

365 Finally we can infer seismicity rate behavior in the presence of both oscillatory stresses
 366 with short periods $S_T^S(t)$ and long periods $S_T^L(t)$ relative to t_a . Inspection of equation
 367 B5 suggests that long period stresses changes act to modulate the background rate. This
 368 suggests a combined form of equations A10 and B5

$$\frac{R(t)}{r} = \frac{\exp(S_T^S(t))}{\frac{1}{M} \left(1 - t_a \frac{S_T^L(t)}{A\sigma_0}\right)}, \quad (\text{B6})$$

369 where M is the long-term mean of $\exp(S_T^S(t))$ i.e. the short period stresses. While equa-
 370 tion B6 is derived here by inspection it can be derived explicitly in the same manner as
 371 equation B5 by assuming that the long period stresses long periods $S_T^L(t)+t/t_a$ can be
 372 considered constant at the time-scale that $\exp(S_T^S(t))$ converges to a mean. This is es-
 373 sentially the same assumption as is required for equations A10 to be valid.

374 References

375 Ader, T. J., Lapusta, N., Avouac, J.-P., & Ampuero, J.-P. (2014, 05). Response of
 376 rate-and-state seismogenic faults to harmonic shear-stress perturbations. *Geo-*

- 377 *physical Journal International*, 198(1), 385-413. doi: 10.1093/gji/ggu144
- 378 Agnew, D. C. (1997). Nloadf: A program for computing ocean-tide loading. *Jour-*
379 *nal of Geophysical Research: Solid Earth*, 102(B3), 5109-5110. doi: 10.1029/
380 96JB03458
- 381 Amos, C. B., Audet, P., Hammond, W. C., Bürgmann, R., Johanson, I. A., & Ble-
382 witt, G. (2014). Uplift and seismicity driven by groundwater depletion in
383 central california. *Nature*, 509(7501), 483–486. doi: 10.1038/nature13275
- 384 Ampuero, J.-P., & Rubin, A. M. (2008). Earthquake nucleation on rate and state
385 faults – aging and slip laws. *Journal of Geophysical Research: Solid Earth*,
386 113(B1). doi: 10.1029/2007JB005082
- 387 Beeler, N. M., & Lockner, D. A. (2003). Why earthquakes correlate weakly with the
388 solid earth tides: Effects of periodic stress on the rate and probability of earth-
389 quake occurrence. *Journal of Geophysical Research: Solid Earth*, 108(B8). doi:
390 10.1029/2001JB001518
- 391 Bettinelli, P., Avouac, J.-P., Flouzat, M., Bollinger, L., Ramillien, G., Rajaure, S., &
392 Sapkota, S. (2008). Seasonal variations of seismicity and geodetic strain in the
393 himalaya induced by surface hydrology. *Earth and Planetary Science Letters*,
394 266(3), 332–344. doi: 10.1016/j.epsl.2007.11.021
- 395 Chanard, K., Nicolas, A., Hatano, T., Petrelis, F., Latour, S., Vinciguerra, S., &
396 Schubnel, A. (2019). Sensitivity of acoustic emission triggering to small pore
397 pressure cycling perturbations during brittle creep. *Geophysical Research*
398 *Letters*, 46(13), 7414-7423. doi: 10.1029/2019GL082093
- 399 Cochran, E. S., Vidale, J. E., & Tanaka, S. (2004). Earth tides can trigger shallow
400 thrust fault earthquakes. *Science*, 306(5699), 1164–1166. doi: 10.1126/science
401 .1103961
- 402 Delorey, A. A., van der Elst, N. J., & Johnson, P. A. (2017). Tidal triggering of
403 earthquakes suggests poroelastic behavior on the san andreas fault. *Earth and*
404 *Planetary Science Letters*, 460, 164 - 170. doi: [https://doi.org/10.1016/j.epsl](https://doi.org/10.1016/j.epsl.2016.12.014)
405 [.2016.12.014](https://doi.org/10.1016/j.epsl.2016.12.014)
- 406 Dieterich, J. (1994). A constitutive law for rate of earthquake production and its
407 application to earthquake clustering. *J. Geophys. Res. Solid Earth*, 99(B2),
408 2601–2618. doi: 10.1029/93JB02581
- 409 Dieterich, J. (2007). 4.04 - applications of rate- and state-dependent friction to

- 410 models of fault-slip and earthquake occurrence. In G. Schubert (Ed.), *Treatise*
411 *on geophysics (second edition)* (Second Edition ed., p. 93 - 110). Oxford: El-
412 sevier. Retrieved from [http://www.sciencedirect.com/science/article/](http://www.sciencedirect.com/science/article/pii/B9780444538024000750)
413 [pii/B9780444538024000750](http://www.sciencedirect.com/science/article/pii/B9780444538024000750) doi: <https://doi.org/10.1016/B978-0-444-53802-4>
414 [.00075-0](https://doi.org/10.1016/B978-0-444-53802-4)
- 415 Duennebieer, F., & Sutton, G. H. (1974). Thermal moonquakes. *Journal of Geophys-*
416 *ical Research (1896-1977)*, 79(29), 4351-4363. doi: 10.1029/JB079i029p04351
- 417 Hainzl, S., Brietzke, G. B., & Zoller, G. (2010). Quantitative earthquake forecasts
418 resulting from static stress triggering. *Journal of Geophysical Research: Solid*
419 *Earth*, 115(B11). doi: 10.1029/2010JB007473
- 420 Hainzl, S., Steacy, S., & Marsan, D. (2010). Seismicity models based on coulomb
421 stress calculations.
- 422 Hawthorne, J. C., & Rubin, A. M. (2010). Tidal modulation of slow slip in casca-
423 dia. *Journal of Geophysical Research: Solid Earth*, 115(B9). doi: 10.1029/
424 2010JB007502
- 425 Heimisson, E. R. (2019). Constitutive law for earthquake production based
426 on rate-and-state friction: Theory and application of interacting sources.
427 *Journal of Geophysical Research: Solid Earth*, 124(2), 1802-1821. doi:
428 10.1029/2018JB016823
- 429 Heimisson, E. R., & Segall, P. (2018). Constitutive law for earthquake production
430 based on rate-and-state friction: Dieterich 1994 revisited. *Journal of Geophys-*
431 *ical Research: Solid Earth*, 123(5), 4141-4156. doi: 10.1029/2018JB015656
- 432 Helmstetter, A., & Shaw, B. E. (2009). Afterslip and aftershocks in the rate-and-
433 state friction law. *Journal of Geophysical Research: Solid Earth*, 114(B1). doi:
434 10.1029/2007JB005077
- 435 Houston, H. (2015). Low friction and fault weakening revealed by rising sensitiv-
436 ity of tremor to tidal stress. *Nature Geoscience*, 8(5), 409-415. doi: 10.1038/
437 ngeo2419
- 438 Johnson, C. W., Fu, Y., & Bürgmann, R. (2017). Seasonal water storage, stress
439 modulation, and california seismicity. *Science*, 356(6343), 1161-1164. doi: 10
440 .1126/science.aak9547
- 441 Johnson, C. W., Fu, Y., & Bürgmann, R. (2020). Hydrospheric modulation of stress
442 and seismicity on shallow faults in southern alaska. *Earth and Planetary Sci-*

- 443 *ence Letters*, 530, 115904. doi: 10.1016/j.epsl.2019.115904
- 444 Kaneko, Y., & Lapusta, N. (2008). Variability of earthquake nucleation in
445 continuum models of rate-and-state faults and implications for aftershock
446 rates. *Journal of Geophysical Research: Solid Earth*, 113(B12). doi:
447 10.1029/2007JB005154
- 448 Linker, M. F., & Dieterich, J. H. (1992). Effects of variable normal stress on rock
449 friction: Observations and constitutive equations. *J. Geophys. Res. Solid
450 Earth*, 97(B4), 4923–4940. doi: 10.1029/92JB00017
- 451 Lognonne, P. (2005). Planetary seismology. *Annual Review of Earth and Planetary
452 Sciences*, 33(1), 571–604. doi: 10.1146/annurev.earth.33.092203.122604
- 453 Lu, Z., Yi, H., & Wen, L. (2018). Loading-induced earth’s stress change over
454 time. *Journal of Geophysical Research: Solid Earth*, 123(5), 4285–4306. doi:
455 10.1029/2017JB015243
- 456 Luo, Y., & Liu, Z. (2019). Slow-slip recurrent pattern changes: Perturba-
457 tion responding and possible scenarios of precursor toward a megathrust
458 earthquake. *Geochemistry, Geophysics, Geosystems*, 20(2), 852–871. doi:
459 10.1029/2018GC008021
- 460 Manga, M., Zhai, G., & Wang, C.-Y. (2019). Squeezing marsquakes out of
461 groundwater. *Geophysical Research Letters*, 46(12), 6333–6340. Retrieved
462 from [https://agupubs.onlinelibrary.wiley.com/doi/abs/10.1029/
463 2019GL082892](https://agupubs.onlinelibrary.wiley.com/doi/abs/10.1029/2019GL082892) doi: 10.1029/2019GL082892
- 464 Milbert, D. (2018). *Solid*. <https://geodesyworld.github.io/SOFTS/solid.htm>.
465 (version update used: 2018-Jun-07)
- 466 Ross, Z. E., Trugman, D. T., Hauksson, E., & Shearer, P. M. (2019). Searching for
467 hidden earthquakes in southern california. *Science*, 364(6442), 767–771. Re-
468 trieved from <https://science.sciencemag.org/content/364/6442/767> doi:
469 10.1126/science.aaw6888
- 470 Rubin, A. M., & Ampuero, J.-P. (2005). Earthquake nucleation on (aging) rate and
471 state faults. *Journal of Geophysical Research: Solid Earth*, 110(B11). doi: 10
472 .1029/2005JB003686
- 473 Rubinstein, J. L., La Rocca, M., Vidale, J. E., Creager, K. C., & Wech, A. G.
474 (2008). Tidal modulation of nonvolcanic tremor. *Science*, 319(5860), 186–
475 189. doi: 10.1126/science.1150558

- 476 Scholz, C. H., Tan, Y. J., & Albino, F. (2019). The mechanism of tidal triggering of
477 earthquakes at mid-ocean ridges. *Nature communications*, *10*(1), 2526. doi: 10
478 .1038/s41467-019-10605-2
- 479 Tanaka, S. (2012). Tidal triggering of earthquakes prior to the 2011 tohoku-oki
480 earthquake (mw 9.1). *Geophysical Research Letters*, *39*(7). doi: 10.1029/
481 2012GL051179
- 482 Tanaka, S., Ohtake, M., & Sato, H. (2002). Evidence for tidal triggering of earth-
483 quakes as revealed from statistical analysis of global data. *Journal of Geophys-
484 ical Research: Solid Earth*, *107*(B10). doi: 10.1029/2001JB001577
- 485 Tanaka, Y., Yabe, S., & Ide, S. (2015). An estimate of tidal and non-tidal modu-
486 lations of plate subduction speed in the transition zone in the tokai district.
487 *Earth, Planets and Space*, *67*(1), 1–11. doi: 10.1186/s40623-015-0311-2
- 488 Thomas, A. M., Bürgmann, R., Shelly, D. R., Beeler, N. M., & Rudolph, M. L.
489 (2012). Tidal triggering of low frequency earthquakes near parkfield, california:
490 Implications for fault mechanics within the brittle-ductile transition. *Journal
491 of Geophysical Research: Solid Earth*, *117*(B5). doi: 10.1029/2011JB009036
- 492 Thomas, A. M., Nadeau, R. M., & Bürgmann, R. (2009). Tremor-tide correlations
493 and near-lithostatic pore pressure on the deep san andreas fault. *Nature*,
494 *462*(7276), 1048–1051. doi: 10.1038/nature08654
- 495 Tolstoy, M., Vernon, F. L., Orcutt, J. A., & Wyatt, F. K. (2002). Breathing of the
496 seafloor: Tidal correlations of seismicity at Axial volcano. *Geology*, *30*(6), 503-
497 506. doi: 10.1130/0091-7613(2002)030<0503:BOTSTC>2.0.CO;2
- 498 Tsuruoka, H., Ohtake, M., & Sato, H. (1995, 07). Statistical test of the tidal trigger-
499 ing of earthquakes: contribution of the ocean tide loading effect. *Geophysical
500 Journal International*, *122*(1), 183-194. doi: 10.1111/j.1365-246X.1995.tb03546
501 .x
- 502 Ueda, T., & Kato, A. (2019). Seasonal variations in crustal seismicity in san-in dis-
503 trict, southwest japan. *Geophysical Research Letters*, *46*(6), 3172–3179. doi: 10
504 .1029/2018GL081789
- 505 Yabe, S., Tanaka, Y., Houston, H., & Ide, S. (2015). Tidal sensitivity of tectonic
506 tremors in nankai and cascadia subduction zones. *Journal of Geophysical Re-
507 search: Solid Earth*, *120*(11), 7587-7605. doi: 10.1002/2015JB012250